Letter

Resonant excitation of plasma waves in a plasma channel

A. J. Ross,[1] J. Chappell,[1] J. J. van de Wetering,[1] J. Cowley,[1] E. Archer,[1] N. Bourgeois,[2] L. Corner,[3] D. R. Emerson,[4] L. Feder,[1] X. J. Gu,[4] O. Jakobsson,[1,*] H. Jones,[3,†] A. Picksley,[1,‡] L. Reid,[3] W. Wang,[1] R. Walczak,[1,5] and S. M. Hooker[1,§]

[1]*John Adams Institute for Accelerator Science and Department of Physics, University of Oxford, Denys Wilkinson Building, Keble Road, Oxford OX1 3RH, United Kingdom*

[2]*Central Laser Facility, STFC Rutherford Appleton Laboratory, Didcot OX11 0QX, United Kingdom*

[3]*Cockcroft Institute for Accelerator Science and Technology, School of Engineering, The Quadrangle, University of Liverpool, Brownlow Hill, Liverpool L69 3GH, United Kingdom*

[4]*Scientific Computing Department, STFC Daresbury Laboratory, Warrington WA4 4AD, United Kingdom*

[5]*Somerville College, Woodstock Road, Oxford OX2 6HD, United Kingdom*

(Received 19 October 2023; accepted 26 February 2024; published 3 April 2024)

We demonstrate resonant excitation of a plasma wave by a train of short laser pulses guided in a preformed plasma channel, for parameters relevant to a plasma-modulated plasma accelerator (P-MoPA). We show experimentally that a train of $N \approx 10$ short pulses, of total energy ~ 1 J, can be guided through 110 mm long plasma channels with on-axis densities in the range 10^{17}–10^{18} cm^{-3}. The spectrum of the transmitted train is found to be strongly red shifted when the plasma period is tuned to the intratrain pulse spacing. Numerical simulations are found to be in excellent agreement with the measurements and indicate that the resonantly excited plasma waves have an amplitude in the range 3–10 GVm^{-1}, corresponding to an accelerator stage energy gain of order 1 GeV.

DOI: 10.1103/PhysRevResearch.6.L022001

In the laser wakefield accelerator (LWFA) [1], a short laser pulse propagating through a plasma excites a trailing Langmuir wave, within which the generated electric fields can be of the order $E_{\mathrm{wb}} = m_{\mathrm{e}} c \omega_p / e$, where $\omega_p = (n_{\mathrm{e}} e^2 / m_{\mathrm{e}} \epsilon_0)^{1/2}$ is the plasma frequency, and n_{e} is the electron density. For electron densities of interest $E_{\mathrm{wb}} \sim 100\,\mathrm{GVm}^{-1}$, some three orders of magnitude greater than is possible in a conventional accelerator. Considerable progress has been made, including, for example, the acceleration of electrons to energies in the GeV range in centimeter-scale accelerator stages [2–10], and the application of LWFAs to driving compact light sources [11,12]. Recently, free-electron laser gain was demonstrated using laser-accelerated electrons [13,14].

To drive a large amplitude Langmuir (or "plasma") wave, the duration τ_L of the laser pulse must satisfy $\tau_L \lesssim T_p/2$, where $T_p = 2\pi/\omega_p$ is the plasma period, corresponding to $\tau_L \lesssim 100$ fs for plasma densities of interest. As a consequence, recent experimental work has been dominated by the use of high energy (joule-scale) chirped-pulse-amplification [15] Ti:sapphire lasers. However, this laser material has a high quantum defect (34%) [16] which limits the pulse repetition rate of high-energy systems to $f_{\mathrm{rep}} \ll 1$ kHz.

An alternative method for driving the plasma wave is to resonantly excite it with a train of low-energy pulses (or a single long, modulated pulse) in which the pulse spacing (or modulation) is matched to T_p. An example of this approach is the plasma beat-wave accelerator (PBWA) [1,17–19], in which two long pulses of frequencies ω_1 and $\omega_2 = \omega_1 + \omega_p$ are combined to form a pulse modulated at ω_p. Beat-wave acceleration of electrons to energies in the 10 MeV range has been reported; of particular relevance to the present work is that by Tochitsky *et al.* [19], who exploited ponderomotive self-guiding over 3 cm to accelerate electrons to 38 MeV at a gradient of $\sim 1\,\mathrm{GVm}^{-1}$.

Interest in resonant wakefield excitation has revived [20] with the development of novel laser technologies, such as thin-disk lasers that can generate joule-scale pulses at f_{rep} in the kilohertz range, with high ($\gtrsim$10%) wall-plug efficiency [21]. The picosecond-duration pulses provided by these systems are too long to drive a plasma wave directly, and a second laser frequency separated by ω_p is not currently available to drive a PBWA. A potential solution is the plasma-modulated plasma accelerator (P-MoPA) [22], which comprises three stages: (i) a modulator, in which a long (~ 1 ps), high-energy ($\gtrsim 1$ J) laser pulse is spectrally modulated by the low amplitude plasma wave driven by a short ($\lesssim 100$ fs), low-energy ($\lesssim 100$ mJ) "seed" laser pulse as they copropagate in a plasma channel of on-axis density $n_{\mathrm{e},0}$; (ii) a dispersive optical system that converts the spectral modulation to a train of short pulses spaced by $T_{p,0} = 2\pi\sqrt{m_{\mathrm{e}}\epsilon_0/n_{\mathrm{e},0}e^2}$; (iii) an accelerator stage, also of on-axis density $n_{\mathrm{e},0}$, within which the pulse

*Deceased

†Now at Deutsches Elektronen-Synchrotron DESY, Notkestr. 85, 22607 Hamburg, Germany

‡Now at Lawrence Berkeley National Laboratory, Berkeley, California 94720, USA

§simon.hooker@physics.ox.ac.uk

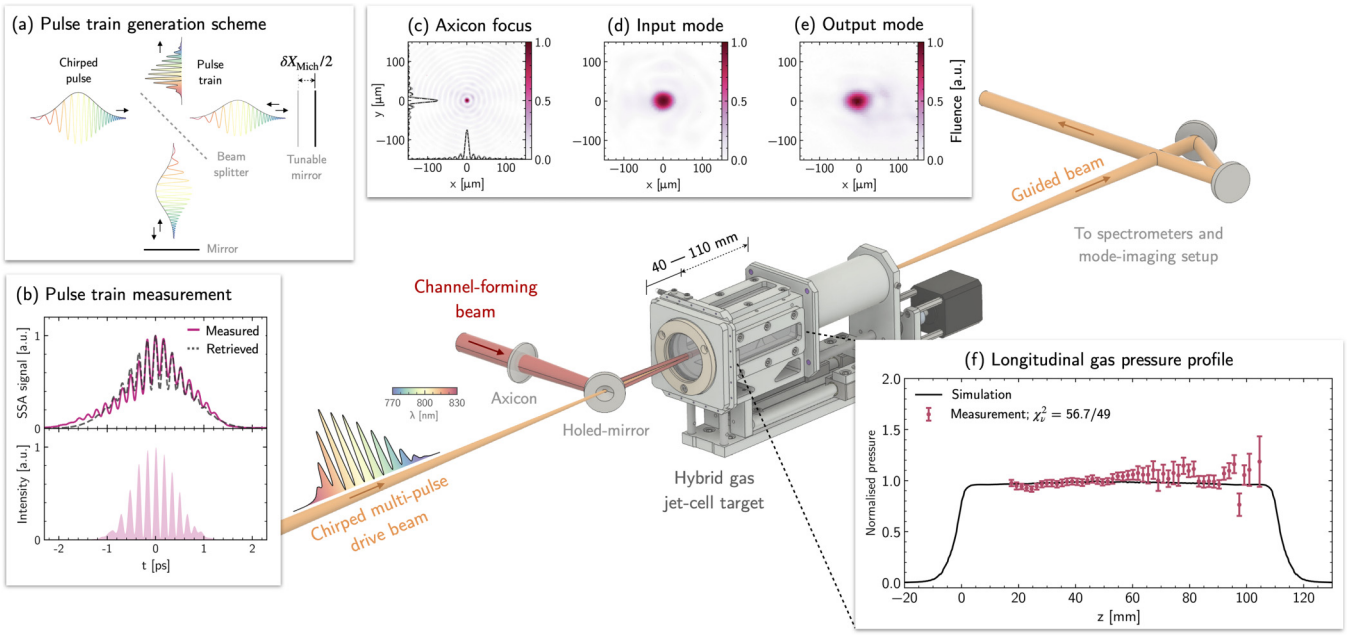

FIG. 1. Sketch of the experimental layout. (a) Illustration of the pulse train generation scheme. (b) Example single-shot autocorrelator (SSA) measurement for the $\tau = (170 \pm 2)$ fs pulse train. Upper: comparison between the measured (pink) and retrieved (gray, dashed) SSA signal. Lower: retrieved pulse train intensity profile. (c) Measured axicon focus. (d) Example input mode of the focused multipulse drive beam. (e) Example guided mode at the channel exit. All focal spot images are normalized to their maximum. (f) Comparison between the measured and simulated longitudinal gas pressure profile [23].

train resonantly drives a large amplitude plasma wave. Numerical simulations [22] show that a 1.7 J, 1 ps driver, with a 140 mJ, 40 fs seed, could accelerate electrons to energies of 0.65 GeV in a 100 mm-long plasma channel with $n_{e,0} = 2.5 \times 10^{17}\,\mathrm{cm}^{-3}$.

In this Letter we investigate experimentally the accelerator stage of a P-MoPA. In order to test the accelerator stage of a P-MoPA in isolation, and since a suitable joule-scale, picosecond-duration laser was not available to us, in this work the pulse train produced by the modulator and compressor stages of a P-MoPA were mimicked by converting a single pulse from a Ti:sapphire laser into a train of short laser pulses. We demonstrate guiding of this train of $N \approx 10$ pulses, with a total energy of the order 1 J through 110 mm long plasma channels, equivalent to 14 Rayleigh ranges, with $n_{e,0}$ in the range 10^{17}–$10^{18}\,\mathrm{cm}^{-3}$. Resonant excitation of a plasma wave within the channel is evidenced by the observation of strong red shifting of the spectrum of the transmitted pulse train when $T_{p,0}$ was tuned to the pulse spacing in the train. The results are found to be in excellent agreement with numerical simulations, which show that wake amplitudes in the range $3\,\mathrm{GVm}^{-1}$ to $10\,\mathrm{GVm}^{-1}$ were achieved, corresponding to an accelerator stage energy gain of the order 1 GeV.

Figure 1 shows schematically the arrangement employed for these experiments, undertaken with the Astra-Gemini TA3 Ti:sapphire laser at the Rutherford Appleton Laboratory. This laser provides two synchronized beams, here denoted the "drive" and "channel-forming" beams, each of central wavelength $\lambda_0 = 800$ nm with transform-limited full-width at half-maximum (FWHM) duration of 31 fs. In order to mimic the pulse train employed in the P-MoPA scheme, single laser pulses were converted to a train of short pulses using a Michelson interferometer, as sketched in Fig. 1(a) and described previously [24,25]. The temporal intensity profile of the generated pulse train, shown in Fig. 1(b), was determined from single-shot measurements of the spectrum and autocorrelation of the train (see the Supplemental Material [23] for further details).

The gas target used in this work was a cell-jet hybrid [10,26], with hydrogen gas pulsed into the target via a solenoid valve and two transducers measuring the pressure on shot. The laser pulses were coupled into, and out of, the target via a pair of 3 mm radius coaxial pinholes mounted on: (i) the front of the target and (ii) a motorized plunger that could be moved to adjust the target length L. A relative RMS pressure variation along the laser propagation axis of 4.1% was measured [23], as shown in Fig. 1(e).

A hydrodynamic optical-field-ionized (HOFI) channel [27,28] was formed in the target by focusing the channel-forming pulse, of energy ~ 100 mJ and FWHM pulse duration 80 fs, with an axicon lens of base angle 3.6°. The transverse intensity profile of the beam produced by the axicon had a central maximum of FWHM spot size (9.8 ± 0.1) μm, as shown in Fig. 1(c).

The pulse train, of total on-target energy $E_{\mathrm{train}} = (2.5 \pm 0.5)$ J, was focused by an off-axis $f/40$ paraboloid to the target entrance. The transverse intensity profile of the focused beam [see Fig. 1(d)] was found to have a $1/e^2$ intensity radius of (45.5 ± 3.4)μm, a Rayleigh range of $z_R = (7.9 \pm 0.7)$ mm, and to contain (64.9 ± 1.5)% of its energy within its FWHM. The delay between the arrival of the channel-forming and drive beams was set to $t_d = 3.5$ ns. After leaving the

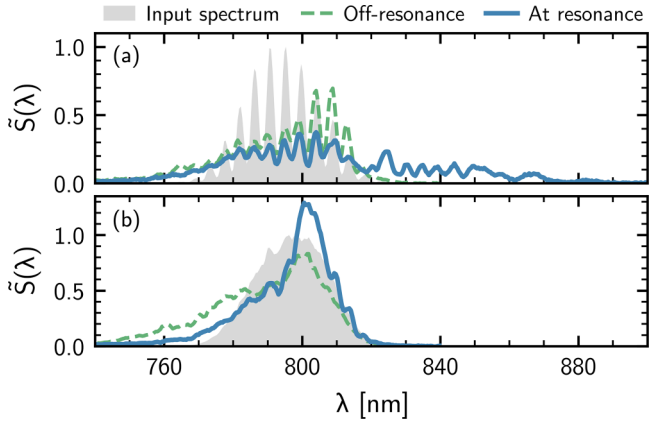

FIG. 2. Comparison of the photon-normalized spectra, $\tilde{S}(\lambda)$, of the input pulses (gray) and those transmitted through a 110 mm-long HOFI channel for (a) a pulse train with $\tau = 170$ fs and $E_{\text{train}} = (2.5 \pm 0.5)$ J; (b) an unmodulated pulse with FWHM duration ~ 1 ps and $E = (2.7 \pm 0.5)$ J. $\tilde{S}(\lambda)$ is shown near the resonance condition of the pulse train [blue; $n_{\text{e,res}} = (4.3 \pm 0.3) \times 10^{17}\,\text{cm}^{-3}$] and for an off-resonant density [green, dashed; $n_{\text{e},0} = (1.4 \pm 0.3) \times 10^{17}\,\text{cm}^{-3}$]. The photon-normalized spectra have been scaled to a maximum value of unity for the input pulse.

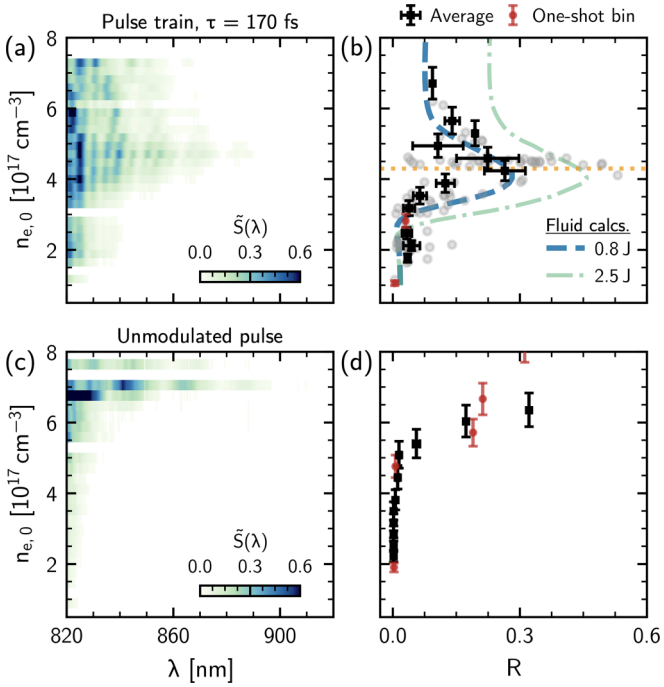

FIG. 3. Density dependence of $\tilde{S}(\lambda)$ for: (a), (b) a pulse train with $\tau = 170$ fs, $E_{\text{train}} = (2.5 \pm 0.5)$ J; and (c), (d) an unmodulated ~ 1 ps, (2.7 ± 0.5) J pulse. (a) and (c): $\tilde{S}(\lambda)$, averaged in electron density bins of width $\Delta n_{\text{e},0} = 0.24 \times 10^{17}\,\text{cm}^{-3}$. (b) and (d): mean values of R [black squares] weighted by energy transmission; red circles indicate bins containing data from only a single shot. The $n_{\text{e},0}$-error bars are a combination of the uncertainties in the measured pressure and the on-axis density calibration. The R-error bars represent the standard error on the mean. In (b), individual data points are plotted (gray circles) and the orange dotted line represents $n_{\text{e,res}}(\tau = 170\,\text{fs})$. Overlaid are the results of the fluid calculations for $E_{\text{train}} = 2.5$ J (green) and $E_{\text{train}} = 0.8$ J (blue).

plasma channel, the energy of the drive beam was reduced, and the beam reimaged onto a 16-bit camera and a fiber-coupled spectrometer. An example guided mode is shown in Fig. 1(e).

The excitation of plasma waves by the drive pulse was detected through changes in its spectrum [29]. The spectra presented in Figs. 2 and 3 are photon normalized, defined as $\tilde{S}(\lambda) = \lambda S_{\text{meas}}(\lambda)/\int_0^\infty \lambda S_{\text{meas}}(\lambda) d\lambda$, where $S_{\text{meas}}(\lambda)$ is the measured spectrum. Figure 2(a) shows $\tilde{S}(\lambda)$ for an incident pulse train with total energy in the pulse train $E_{\text{train}} = (2.5 \pm 0.5)$ J and temporal pulse spacing $\tau = 170$ fs, at on-axis densities approximately equal to, and one third of, the resonant value, $n_{\text{e,res}} \approx 4.3 \times 10^{17}\,\text{cm}^{-3}$. As expected, the input spectrum of the pulse train is modulated by the Michelson interferometer to yield $N \approx 10$ uniformly spaced peaks. For the off-resonant density, the spectrum of the transmitted train is similar to that of the incident pulse, with some blue shifting apparent in the region $\lambda \lesssim 780$ nm, likely caused by ionization of the neutral gas collar [30,31] surrounding the HOFI channel and of the gas plumes that extend beyond the target. In contrast, at the resonant density, considerable red shifting is observed, extending the bandwidth of the input beam by more than 40 nm on the long wavelength side. The new red-shifted light beyond 820 nm is seen to consist of a series of peaks [22]; these arise from spectral modulation of the laser pulse by the wakefield, which generates copies of the input spectrum shifted by $\pm m\omega_p$ for integer m. The peaks on the blue side of the spectrum are not visible in Fig. 2, likely due to the additional blue shift from ionization. We note that blue shifting would have predominantly occurred for the first few pulses in the train, and, since the pulse train was negatively chirped, their initial spectra were on the blue side of the mean wavelength.

The density-dependent red shift seen in Fig. 2(a) strongly indicates resonant plasma wave excitation in the plasma channel. To confirm this, we also measured the transmitted spectra for a temporally smooth ~ 1 ps drive pulse of similar energy at on-axis densities matching those in Fig. 2(a). As shown in Fig. 2(b), in this case no red shift was observed, and the spectra were similar for both densities and were dominated by blue shift of similar magnitude to that observed in Fig. 2(a).

Figure 3 shows the variation with on-axis plasma density of the transmitted spectra when the drive was well guided [23] by the plasma channel. To quantify the red shift we define the red-shift metric $R = \sum_{\lambda_{\text{min}}}^{\infty} \tilde{S}(\lambda)$, where λ_{min} is the longest wavelength in the input spectrum above the noise level. It is evident from Figs. 3(a) and 3(b) that the spectra of the pulse train driver exhibits a pronounced red shift for densities in the range $n_{\text{e},0} = 4 - 5 \times 10^{17}\,\text{cm}^{-3}$, which agrees with the expected resonance density of $n_{\text{e,res}} = 4.3 \times 10^{17}\,\text{cm}^{-3}$. For a train of N identical laser pulses, the full width of the resonance peak is expected [25] to be $\delta n_{\text{e},0}/n_{\text{e,res}} \approx 8/(3N)$, corresponding to $\delta n_{\text{e},0} \approx 1.2 \times 10^{17}\,\text{cm}^{-3}$—in good agreement with the measured FWHM in R of $\delta n_{\text{e},0} \approx 1.6 \times 10^{17}\,\text{cm}^{-3}$. In contrast, Figs. 3(c) and 3(d) show that no resonance is observed for the unmodulated drive pulse. Significant red shifting of the unmodulated drive pulse *is* observed for $n_{\text{e},0} \gtrsim 5.5 \times 10^{17}\,\text{cm}^{-3}$, likely caused by self-modulation [32–34] of the long pulse.

To provide further insight, we compared these measurements with the results of an in-house 2D cylindrical fluid code, benchmarked against the particle-in-cell (PIC) code WARPX [35] (see [23]). The calculations used the retrieved pulse train parameters and modeled the plasma channel as an ideal fully ionized parabolic waveguide [23]. The code ignores the effects of ionization by the laser pulse, and assumes that the temporal envelope of the drive is unchanged by its interaction with the plasma, and hence the code cannot model self-modulation of the pulse.

Figure 3(b) shows the calculated R for the $\tau = 170\,\mathrm{fs}$, $E_{\mathrm{train}} = 2.5\,\mathrm{J}$ pulse train in a plasma channel of length $L = 110\,\mathrm{mm}$. It can be seen that the position and width of the calculated resonance peak agree closely with those observed in the measurements. For some shots the measured R values reach the calculated curve, but in most cases they are lower. In order to understand this, the energy transmission of the train was measured as a function of the plasma channel length [23]. For each cell length the measured energy transmission was found to vary over a wide range, owing to the large pointing jitter of the input pulse train. Shots for which the input beam was well aligned with the channel axis were found to have an input coupling of $T_0 = (64 \pm 4)\%$, which is consistent with $|c_0|^2 = (71 \pm 5)\%$, where c_0 is the calculated [23] coupling coefficient between the transverse amplitude profile of the input beam and that of the lowest-order mode of the channel. In contrast, the coupling coefficient deduced from all guided shots is only $T_0 = (32 \pm 13)\%$, which reflects the additional losses arising from misalignment with respect to the channel axis. Figure 3(b) shows that if the drive energy is reduced by this factor, i.e., to $E_{\mathrm{train}} = 800\,\mathrm{mJ}$, the calculated variation of R with density is in excellent agreement with the averaged measurements. At the resonant density, the amplitude of the wakefield driven by the $\tau = 170\,\mathrm{fs}$ pulse train is calculated from the fluid simulation to be $10\,\mathrm{GVm^{-1}}$ ($3\,\mathrm{GVm^{-1}}$) for $E_{\mathrm{train}} = 2.5\,\mathrm{J}$ ($0.8\,\mathrm{J}$).

Further evidence of resonant wakefield excitation is shown in Fig. 4, which shows the measured and calculated variation of R with on-axis density for pulse trains with $\tau = 200\,\mathrm{fs}$ and 170 fs. In this case, $E_{\mathrm{train}} = (2.5 \pm 0.5)\,\mathrm{J}$ and $L = 70\,\mathrm{mm}$. It can be seen that, for both pulse trains, the position, width, and magnitude of the measured variation of R are consistent with the calculation assuming $E_{\mathrm{train}} = 0.8\,\mathrm{J}$. At higher densities, $n_{\mathrm{e},0} \gtrsim 7 \times 10^{17}\,\mathrm{cm^{-3}}$, red shifting arising from self-modulation is again observed.

It has been previously shown that HOFI [27,28] channels achieve higher energy transmission when the wings of the laser pulse have sufficient intensity to ionize the neutral gas collar to form a conditioned [36,37] HOFI channel. PIC simulations [23] of the present experiment indicate that the leading three pulses in the train conditioned the HOFI channel, allowing later pulses in the train to be guided with low losses. We note that conditioning of the channel could also be achieved by employing a separate, short pulse immediately ahead of the pulse train [30]; the required energy of the conditioning pulse is $\sim 7\,\mathrm{mJ}$ per cm of the channel, i.e., only 3% of the drive energy in the present experiment.

In summary we have demonstrated guiding of a train of $N \approx 10$ short pulses, with a total pulse train energy of the order 1 J through 110 mm long plasma channels with on-axis densities in the range 10^{17}–$10^{18}\,\mathrm{cm^{-3}}$. The spectra of the transmitted pulse trains were found to be strongly red shifted when the plasma period was matched to the pulse spacing in the train. In contrast, no such resonance in the red shift was observed for an unmodulated drive pulse of the same total energy and duration. Numerical simulations were found to be in excellent agreement with the measurements, and showed that, at resonance, the wake amplitude was in the range $3 - 10\,\mathrm{GVm^{-1}}$, corresponding to an accelerator stage energy gain of the order 1 GeV.

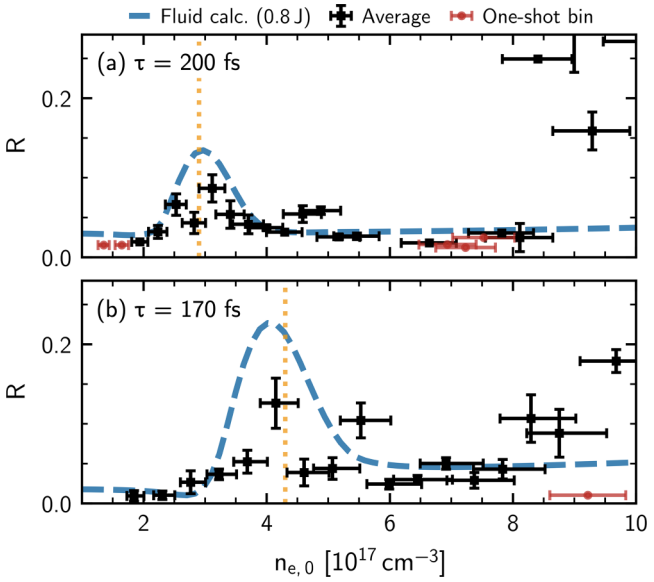

FIG. 4. Variation of R with on-axis density for a plasma channel of length $L = 70\,\mathrm{mm}$ and for pulse trains of energy $(2.7 \pm 0.5)\,\mathrm{J}$ and pulse separation: (a) $\tau = 200\,\mathrm{fs}$ and (b) $\tau = 170\,\mathrm{fs}$. The results of the fluid calculations, assuming $E_{\mathrm{train}} = 800\,\mathrm{mJ}$, are shown by the blue dashed lines. For each plot the expected resonant density is indicated by the orange dotted line.

These results constitute the first demonstration of resonant excitation of a plasma wave by a train of laser pulses guided in a preformed plasma channel. The laser and plasma parameters employed in this work are directly relevant to the accelerator stage of the P-MoPA scheme [22], which offers a route to achieving kilohertz-repetition-rate, GeV-scale plasma accelerators driven by plasma modulation of joule-scale, picosecond-duration laser pulses, such as those provided by thin-disk lasers.

Data is available at [44].

This research was funded in whole, or in part, by EPSRC and STFC, which are Plan S funders.

Acknowledgments. This work was supported by the UK Engineering and Physical Sciences Research Council (EPSRC) (Grants No. EP/R513295/1 and No. EP/V006797/1), the UK Science and Technologies Facilities Council (Grants No. ST/P002048/1, No. ST/R505006/1, No. ST/S505833/1, No. ST/V001655/1, and No. ST/V001612/1), and the Ken and Veronica Tregidgo Scholarship in Atomic and Laser Physics. This work required significant computing resources

which were funded by the plasma HEC Consortium [EPSRC Grant No. EP/R029149/1] and UKRI funding [ARCHER2 Pioneer Projects]. Computing resources were provided by ARCHER and ARCHER2 [ARCHER2 PR17125] UK supercomputers [45,46] . This research used the open-source particle-in-cell code WARPX [47], primarily funded by the US DOE Exascale Computing Project. Primary WARPX contributors are with LBNL, LLNL, CEA-LIDYL, SLAC, DESY, CERN, and TAE Technologies. We acknowledge all WARPX contributors.

[1] T. Tajima and J. M. Dawson, Laser electron accelerator, Phys. Rev. Lett. **43**, 267 (1979).

[2] W. P. Leemans, B. Nagler, A. J. Gonsalves, C. Tóth, K. Nakamura, C. G. R. Geddes, E. Esarey, C. B. Schroeder, and S. M. Hooker, GeV electron beams from a centimetre-scale accelerator, Nat. Phys. **2**, 696 (2006).

[3] S. Kneip, S. R. Nagel, S. F. Martins, S. P. D. Mangles, C. Bellei, O. Chekhlov, R. J. Clarke, N. Delerue, E. J. Divall, G. Doucas, K. Ertel, F. Fiuza, R. Fonseca, P. Foster, S. J. Hawkes, C. J. Hooker, K. Krushelnick, W. B. Mori, C. A. J. Palmer, K. TaPhuoc *et al.*, Near-GeV acceleration of electrons by a nonlinear plasma wave driven by a self-guided laser pulse, Phys. Rev. Lett. **103**, 035002 (2009).

[4] X. Wang, R. Zgadzaj, N. Fazel, Z. Li, S. A. Yi, X. Zhang, W. Henderson, Y. Y. Chang, R. Korzekwa, H. E. Tsai, C. H. Pai, H. Quevedo, G. Dyer, E. Gaul, M. Martinez, A. C. Bernstein, T. Borger, M. Spinks, M. Donovan, V. Khudik *et al.*, Quasi-monoenergetic laser-plasma acceleration of electrons to 2 GeV, Nat. Commun. **4**, 1988 (2013).

[5] W. P. Leemans, A. J. Gonsalves, H.-S. Mao, K. Nakamura, C. Benedetti, C. B. Schroeder, C. Tóth, J. Daniels, D. E. Mittelberger, S. S. Bulanov, J.-L. Vay, C. G. R. Geddes, and E. Esarey, Multi-GeV electron beams from capillary-discharge-guided subpetawatt laser pulses in the self-trapping regime, Phys. Rev. Lett. **113**, 245002 (2014).

[6] J. Shin, H. T. Kim, V. B. Pathak, C. Hojbota, S. K. Lee, J. H. Sung, H. W. Lee, J. W. Yoon, C. Jeon, K. Nakajima, F. Sylla, A. Lifschitz, E. Guillaume, C. Thaury, V. Malka, and C. H. Nam, Quasi-monoenergetic multi-GeV electron acceleration by optimizing the spatial and spectral phases of PW laser pulses, Plasma Phys. Controlled Fusion **60**, 064007 (2018).

[7] A. J. Gonsalves, K. Nakamura, J. Daniels, C. Benedetti, C. Pieronek, T. C. H. de Raadt, S. Steinke, J. H. Bin, S. S. Bulanov, J. van Tilborg, C. G. R. Geddes, C. B. Schroeder, C. Tóth, E. Esarey, K. Swanson, L. Fan-Chiang, G. Bagdasarov, N. Bobrova, V. Gasilov, G. Korn *et al.*, Petawatt laser guiding and electron beam acceleration to 8 GeV in a laser-heated capillary discharge waveguide, Phys. Rev. Lett. **122**, 084801 (2019).

[8] B. Miao, J. E. Shrock, L. Feder, R. C. Hollinger, J. Morrison, R. Nedbailo, A. Picksley, H. Song, S. Wang, J. J. Rocca, and H. M. Milchberg, Multi-GeV electron bunches from an all-optical laser wakefield accelerator, Phys. Rev. X **12**, 031038 (2022).

[9] K. Oubrerie, A. Leblanc, O. Kononenko, R. Lahaye, I. A. Andriyash, J. Gautier, J.-P. Goddet, L. Martelli, A. Tafzi, K. Ta Phuoc, S. Smartsev, and C. Thaury, Controlled acceleration of GeV electron beams in an all-optical plasma waveguide, Light: Sci. Appl. **11**, 180 (2022).

[10] A. Picksley, J. Chappell, E. Archer, N. Bourgeois, J. Cowley, D. R. Emerson, L. Feder, X. J. Gu, O. Jakobsson, A. J. Ross, W. Wang, R. Walczak, and S. M. Hooker, All-optical GeV electron bunch generation in a laser-plasma accelerator via truncated-channel injection, Phys. Rev. Lett. **131**, 245001 (2023).

[11] S. Corde, K. Ta Phuoc, G. Lambert, R. Fitour, V. Malka, A. Rousse, A. Beck, and E. Lefebvre, Femtosecond x rays from laser-plasma accelerators, Rev. Mod. Phys. **85**, 1 (2013).

[12] F. Albert and A. G. R. Thomas, Applications of laser wakefield accelerator-based light sources, Plasma Phys. Controlled Fusion **58**, 103001 (2016).

[13] W. Wang, K. Feng, L. Ke, C. Yu, Y. Xu, R. Qi, Y. Chen, Z. Qin, Z. Zhang, M. Fang, J. Liu, K. Jiang, H. Wang, C. Wang, X. Yang, F. Wu, Y. Leng, J. Liu, R. Li, and Z. Xu, Free-electron lasing at 27 nanometres based on a laser wakefield accelerator, Nature (London) **595**, 516 (2021).

[14] M. Labat, J. C. Cabadağ, A. Ghaith, A. Irman, A. Berlioux, P. Berteaud, F. Blache, S. Bock, F. Bouvet, F. Briquez, Y.-Y. Chang, S. Corde, A. Debus, C. D. Oliveira, J.-P. Duval, Y. Dietrich, M. E. Ajjouri, C. Eisenmann, J. Gautier, R. Gebhardt *et al.*, Seeded free-electron laser driven by a compact laser plasma accelerator, Nat. Photon. **17**, 150 (2023).

[15] D. Strickland and G. Mourou, Compression of amplified chirped optical pulses, Opt. Commun. **56**, 219 (1985).

[16] C. W. Siders, T. Galvin, A. Erlandson, A. Bayramian, B. Reagan, E. Sistrunk, T. Spinka, and C. Haefner, Wavelength scaling of laser wakefield acceleration for the EuPRAXIA design point, Instruments **3**, 44 (2019).

[17] C. Joshi, W. B. Mori, T. Katsouleas, J. M. Dawson, J. M. Kindel, and D. W. Forslund, Ultrahigh gradient particle-acceleration by intense laser-driven plasma-density waves, Nature (London) **311**, 525 (1984).

[18] C. E. Clayton, K. A. Marsh, A. Dyson, M. Everett, A. Lal, W. P. Leemans, R. Williams, and C. Joshi, Ultrahigh-gradient acceleration of injected electrons by laser-excited relativistic electron plasma waves, Phys. Rev. Lett. **70**, 37 (1993).

[19] S. Y. Tochitsky, R. Narang, C. V. Filip, P. Musumeci, C. E. Clayton, R. B. Yoder, K. A. Marsh, J. B. Rosenzweig, C. Pellegrini, and C. Joshi, Enhanced acceleration of injected electrons in a laser-beat-wave-induced plasma channel, Phys. Rev. Lett. **92**, 095004 (2004).

[20] S. M. Hooker, R. Bartolini, S. P. D. Mangles, A. Tünnermann, L. Corner, J. Limpert, A. Seryi, and R. Walczak, Multi-pulse laser wakefield acceleration: A new route to efficient, high-repetition-rate plasma accelerators and high flux radiation sources, J. Phys. B: At., Mol. Opt. Phys. **47**, 234003 (2014).

[21] Y. Wang, H. Chi, C. Baumgarten, K. Dehne, A. R. Meadows, A. Davenport, G. Murray, B. A. Reagan, C. S. Menoni, and J. J. Rocca, 11 J Yb:YAG picosecond laser at 1 kHz repetition rate, Opt. Lett. **45**, 6615 (2020).

[22] O. Jakobsson, S. M. Hooker, and R. Walczak, Gev-scale accelerators driven by plasma-modulated pulses from kilohertz lasers, Phys. Rev. Lett. **127**, 184801 (2021).

[23] See Supplemental Material at http://link.aps.org/supplemental/10.1103/PhysRevResearch.6.L022001 for further details on the experimental setup, pulse train diagnosis, and guiding measurements which includes Refs. [38–43].

[24] R. Shalloo, L. Corner, C. Arran, J. Cowley, G. Cheung, C. Thornton, R. Walczak, and S. Hooker, Generation of laser pulse trains for tests of multi-pulse laser wakefield acceleration, Nucl. Instrum. Methods Phys. Res., Sect. A **829**, 383 (2016).

[25] J. Cowley, C. Thornton, C. Arran, R. J. Shalloo, L. Corner, G. Cheung, C. D. Gregory, S. P. D. Mangles, N. H. Matlis, D. R. Symes, R. Walczak, and S. M. Hooker, Excitation and control of plasma wakefields by multiple laser pulses, Phys. Rev. Lett. **119**, 044802 (2017).

[26] C. Aniculaesei, H. T. Kim, B. J. Yoo, K. H. Oh, and C. H. Nam, Novel gas target for laser wakefield accelerators, Rev. Sci. Instrum. **89**, 025110 (2018).

[27] R. J. Shalloo, C. Arran, L. Corner, J. Holloway, J. Jonnerby, R. Walczak, H. M. Milchberg, and S. M. Hooker, Hydrodynamic optical-field-ionized plasma channels, Phys. Rev. E **97**, 053203 (2018).

[28] R. J. Shalloo, C. Arran, A. Picksley, A. von Boetticher, L. Corner, J. Holloway, G. Hine, J. Jonnerby, H. M. Milchberg, C. Thornton, R. Walczak, and S. M. Hooker, Low-density hydrodynamic optical-field-ionized plasma channels generated with an axicon lens, Phys. Rev. Accel. Beams **22**, 041302 (2019).

[29] E. Esarey, A. Ting, and P. Sprangle, Frequency shifts induced in laser pulses by plasma waves, Phys. Rev. A **42**, 3526 (1990).

[30] A. Picksley, A. Alejo, R. J. Shalloo, C. Arran, A. von Boetticher, L. Corner, J. A. Holloway, J. Jonnerby, O. Jakobsson, C. Thornton, R. Walczak, and S. M. Hooker, Meter-scale conditioned hydrodynamic optical-field-ionized plasma channels, Phys. Rev. E **102**, 053201 (2020).

[31] L. Feder, B. Miao, J. E. Shrock, A. Goffin, and H. M. Milchberg, Self-waveguiding of relativistic laser pulses in neutral gas channels, Phys. Rev. Res. **2**, 043173 (2020).

[32] C. E. Max, J. Arons, and A. B. Langdon, Self-modulation and self-focusing of electromagnetic waves in plasmas, Phys. Rev. Lett. **33**, 209 (1974).

[33] E. Esarey, J. Krall, and P. Sprangle, Envelope analysis of intense laser pulse self-modulation in plasmas, Phys. Rev. Lett. **72**, 2887 (1994).

[34] K. Nakajima, D. Fisher, T. Kawakubo, H. Nakanishi, A. Ogata, Y. Kato, Y. Kitagawa, R. Kodama, K. Mima, H. Shiraga, K. Suzuki, K. Yamakawa, T. Zhang, Y. Sakawa, T. Shoji, Y. Nishida, N. Yugami, M. Downer, and T. Tajima, Observation of ultrahigh gradient electron acceleration by a self-modulated intense short laser pulse, Phys. Rev. Lett. **74**, 4428 (1995).

[35] L. Fedeli, A. Huebl, F. Boillod-Cerneux, T. Clark, K. Gott, C. Hillairet, S. Jaure, A. Leblanc, R. Lehe, A. Myers, C. Piechurski, M. Sato, N. Zaim, W. Zhang, J. Vay, and H. Vincenti, Pushing the frontier in the design of laser-based electron accelerators with groundbreaking mesh-refined particle-in-cell simulations on exascale-class supercomputers, in *2022 SC22: International Conference for High Performance Computing, Networking, Storage and Analysis (SC)* (IEEE Computer Society, Dallas, TX, USA, 2022), pp. 1–12, doi:10.1109/SC41404.2022.00008.

[36] A. Picksley, A. Alejo, J. Cowley, N. Bourgeois, L. Corner, L. Feder, J. Holloway, H. Jones, J. Jonnerby, H. M. Milchberg, L. R. Reid, A. J. Ross, R. Walczak, and S. M. Hooker, Guiding of high-intensity laser pulses in 100-mm-long hydrodynamic optical-field-ionized plasma channels, Phys. Rev. Accel. Beams **23**, 081303 (2020).

[37] B. Miao, L. Feder, J. E. Shrock, A. Goffin, and H. M. Milchberg, Optical guiding in meter-scale plasma waveguides, Phys. Rev. Lett. **125**, 074801 (2020).

[38] Y. Fournier, J. Bonelle, C. Moulinec, Z. Shang, A. Sunderland, and J. Uribe, Optimizing *Code_Saturne* computations on petascale systems, Comput. Fluids **45**, 103 (2011).

[39] F. Archambeau, N. Méchitoua, and M. Sakiz, Code Saturne: A Finite Volume Code for the computation of turbulent incompressible flows - Industrial Applications, International Journal on Finite Volumes **1**, 1 (2004).

[40] G. J. McLachlan and D. Peel, *Finite mixture models*, Wiley Series in Probability and Statistics (John Wiley & Sons, Inc, New York City, 2000).

[41] H. Akaike, Information theory and an extension of the maximum likelihood principle, in *Selected Papers of Hirotugu Akaike*, edited by E. Parzen, K. Tanabe, and G. Kitagawa (Springer, New York, NY, 1998), pp. 199–213.

[42] J. J. van de Wetering, S. M. Hooker, and R. Walczak, Stability of the modulator in a plasma-modulated plasma accelerator, Phys. Rev. E **108**, 015204 (2023).

[43] M. V. Ammosov, N. B. Delone, and V. P. Krainov, Tunnel ionization of complex atoms and of atomic ions in an alternating electromagnetic field, J. Exp. Theor. Phys. **64**, 1191 (1986).

[44] A. J. Ross, Resonant excitation of plasma waves in a plasma channel - data 2024, doi:10.5281/zenodo.10865431.

[45] http://archer.ac.uk.

[46] https://www.archer2.ac.uk.

[47] https://github.com/ECP-WarpX/WarpX.